JJMIE

Volume 19, Number 2, June. 2025
ISSN 1995-6665
Pages 249– 262
https://doi.org/10.59038/jjmie/190201
Editor-in-Chief: Prof. Ali M. Jawarneh

Jordan Journal of Mechanical and Industrial Engineering

CFD Based Design Optimization of Convergent-Divergent Nozzle of High-Speed Rocket Using the Taguchi Method for Enhanced Flow Characteristics

Syed Masood Arif Bukhari [a], Bushra Meraj [b], Naveed Husnain [a,*], Rashida Qurashi [b], Waseem Abbas [c], Muhammad Tuoqeer Anwar [d], Nida Wajahat [e], Ali Tahir [f], Muhammad Farooq Zaman [a]

[a]Department of Mechanical Engineering, Faculty of Engineering and Technology, Bahauddin Zakariya University, Multan 60800, Pakistan.
[b]Government Graduate College for Women, Makhdoom Rasheed Multan 59100, Pakistan.
[c]Institute of Physics, Bahauddin Zakariya University, 60800 Multan, Pakistan.
[d]Department of Mechanical Engineering, COMSATS University Islamabad, Sahiwal Campus, Off G.T. Road, Sahiwal 57000, Pakistan.
[e]Department of Computer Science, Government Associate College for Women Kabirwala, Khanewal 58250, Pakistan.
[f]College of Electrical and Mechanical Engineering, National University of Sciences and Technology, H-12, 44000 Islamabad, Pakistan.

Received 2 Jan 2025 *Accepted 19 Mar 2025*

Abstract

Convergent-divergent (C-D) nozzles are widely used in the aerospace industry to produce thrust at the exit by increasing the velocity and converting the subsonic flow of gases at the inlet into supersonic flow at the outlet. For enhanced flow characteristics, the design of C-D nozzles must be optimized. In this study, the design parameters of the C-D nozzle of a high-speed rocket i.e. throat diameter, convergent angle, and divergent angle are optimized using the Taguchi method. Design of Experiments (DOE)is performed based on Taguchi's L9 orthogonal array by altering the above-mentioned design parameters at three levels. Based on DOE, the nozzles are designed using SolidWorks, and Computational Fluid Dynamics (CFD) analysis is performed on ANSYS. The response flow characteristics i.e. exit Mach number, exit velocity, and exit pressure (calculated through simulations) are analyzed using the Taguchi method to find the optimized set of parameters. The results depict that shock waves appear in some of the nozzle models from DOE. Other nozzles without shock waves provide perfect supersonic flow at the outlet of the rocket nozzle by increasing the velocity and reducing the pressure. The maximum Mach number at the outlet of the C-D nozzle for the given DOE is 3.45 for the given design, a smaller throat diameter provides better results. Based on Taguchi's S/N ratio analysis, the optimized set of design parameters that can give a high Mach number at the outlet, high velocity at the outlet, and low pressure at the outlet, is 0.304 m throat diameter, 28° convergent angle and 20° divergent angle.

Keywords: CFD, CD Nozzle, Design Optimization, Flow Characteristics, ANSYS CFX, Rocket, Aerospace.

1. Introduction

Convergent-divergent (C-D) nozzles also known as de Laval nozzles, have two sections i.e. convergent and divergent sections as their name suggests, with an intermediate section, known as throat. C-D nozzles are primarily used in jet engines and rockets to increase the velocity at the exit. Hot gases have high temperatures and pressure inside the combustion chamber which, after entering in C-D nozzle, decrease at the expense of velocity[1]. The flow of exhaust gases at the inlet of the C-D nozzle is subsonic and remains subsonic in the convergent section. The flow becomes sonic at the throat of the C-D nozzle i.e. Mach number becomes equal to 1 if the nozzle is choked. In the divergent portion, the Mach number increases along with velocity and flow becomes supersonic, i.e., the Mach number is greater than 1. The core purpose of the C-D nozzle is to increase the flow of combustion gases and produce a thrust at the outlet. Sometimes, shock waves can appear in the flow across the nozzle which causes the Mach number to decrease when reaching supersonic conditions. Shock waves are typically associated with supersonic flows but in certain conditions, shock waves can also appear in subsonic regimes. Due to shock, the flow at the outlet becomes subsonic or remains supersonic but the Mach number decreases. The flow without shock can be treated as isentropic given that the flow is inviscid and adiabatic. The flow characteristics of exhaust gases inside the nozzle are directly dependent on the design of the C-D nozzle[2]. To optimize the design of the C-D nozzle and to analyze the flow characteristics

* Corresponding author e-mail: naveedhusnain@bzu.edu.pk.

inside the C-D nozzle, the process of experimentation is costly. To overcome this, computational analysis of flow (termed as Computational Fluid Dynamics (CFD)) inside a C-D nozzle is performed for the initial working[3, 4].

Due to its significance, the researchers are analyzing different aspects (including the flow characteristics, design, performance, etc.) of the C-D nozzle. For instance, Zhu and Jiang [5]studied the shock wave length of C-D nozzles. They developed an analytical model for the prediction of shock wavelength. During the comparison, they reported that the results of the analytical model were close to the experimental results with a difference of 11%.In another study, Papamoschou et al.[6] studied the separation of supersonic flow in C-D nozzles. They varied the area ratio from 1 to 6 and pressure ratio from 1.2 to 1.8.They reported that with the increase in area ratio and pressure ratio, the shock developed two lambda feet.Al-Ajlouni[7] proposed an automated method to create the profile of supersonic C-D nozzles.

As mentioned before, CFD analysis is widely used to predict the flow characteristics of fluids[8].It has been successfully applied to predict the flow and performance characteristics of the C-D nozzle. Kumar and Devarajan[9] designed and analyzed a nozzle using CFD in 2D. They designed a C-D nozzle using the geometry modeler in ANSYS and analyzed the nozzle in the ANSYS Fluent module. By analyzing the velocity, pressure, and temperature, they reported that their design provided better results in terms of velocity and temperature. In another study, Nakagawa et al.[10] investigated the supersonic flow of CO_2 in a C-D nozzle. They varied the divergent angle and studied the decompression behavior. For divergent angles >0.306^o for high inlet temperatures, the decompression curve approached the predicted values through Isentropic Homogeneous Equilibrium theory. Jingwei and Elbel[11] performed CFD simulations on R134a flow inside the C-D nozzle. During the simulation, the vortex forced the vapor bubbles in the direction of the center of the nozzle which ultimately enhanced the pressure drop in the divergent portion. Whereas in flow having no vortex, the void fraction in the center remained deceased. Moreover, the mass flow rate with the introduction of a vortex decreased.

Zhalehrajabi et al.[12] investigated the effect of the mesh grid and turbulence model on the convective heat transfer of the C-D nozzle. The coefficient of heat transfer obtained from CFD simulations was compared with the experimental data and the simulated results agreed with the experimental data. Further, Das et al.[13] analyzed the flow behavior inside the C-D nozzle using CFD. Using the properties of compressible flow, they investigated the Mach number, velocity, pressure, and density of flows inside the C-D nozzle. At some pressures, abnormal behavior of output parameters was shown due to shockwaves. Furthermore, similar studies also focused on flow behavior at different Mach numbers [14, 15]. Douaiba et al.[16] also analyzed the compressible flow at the outlet of the C-D nozzle. Khan et al.[17] investigated the compressible flow in a C-D nozzle using CFD analysis. They analyzed the 2D flow of air inside a supersonic C-D nozzle. ANSYS Fluent module was used to simulate the flow. The simulations were done based on three nozzle pressure ratios i.e. 6, 7.82, and 8.2. The results demonstrated that CFD can be a good option to simulate shock patterns inside a duct to provide flow information. In another instance, Vadiveluet al.[18] also analyzed the performance of the C-D nozzle. They selected a rocket nozzle and performed CFD analysis on that nozzle. Keeping the other input parameters constant, they altered the back pressures of the nozzle to investigate the performance under different back pressures. They reported the optimal back pressure value to be 0.864 bar.

Flow properties of the C-D nozzle are linked directly with the design aspects of the nozzle. Madhu et al.[19] investigated the flow properties of a C-D nozzle using different divergent angles. They utilized the ANSYS Fluent module to assess the flow properties of gases. Mach number, static pressure, and velocity were assessed during the simulation. They varied divergence angle at three stages i.e. 9, 11, and 13 degrees. The results demonstrated that shocks were absent in the flows having higher divergent angles. Taking this work further, Meena et al.[2]also varied throat diameter as well along with the divergent angle. Divergent angles were varied at five stages i.e. 10, 12, 14, 16, and 18 degrees. Moreover, two throat diameters were analyzed i.e. 0.304 and 0.404 meters. The C-D nozzles were designed in SolidWorks and analyzed in ANSYS Fluent. This too validated the results presented by Madhu et al. which have been mentioned earlier. With a throat diameter of 0.404 m, the maximum velocity recorded was 1500 m/s whereas with 0.303 m, the maximum velocity was 1900 m/s. This provided the idea that increasing throat diameter can alter the exit velocity depending on the flow regime. Kore et al.[20] altered the convergence angles of the C-D nozzle by keeping the divergence angle and throat diameter constant. Convergence angles were varied as 40, 45, 50, and 55 degrees, and using CFD, Mach number, velocity, and pressures were assessed. Aabid and Khan[21] analyzed the C-D nozzle by using a combination of CFD and Design of Experiments (DOE).

The present study drives the work a step further. Three design parameters, i.e. convergent angle, divergent angle, and throat diameter are varied at the same time to analyze their effect on the flow characteristics (velocity, pressure, and Mach number) of a rocket C-D nozzle. The scope of the study is not just limited to this, but it proposes an optimal design condition of the C-D nozzle for high-speed rockets that can provide better flow characteristics. The design optimization is done through Taguchi's DOE. L9 array is presented in this study by varying the design parameters to three levels each. Based on DOE, nozzles were designed in SolidWorks, and CFD simulations were performed using the CFX module of ANSYS Workbench to analyze the outlet Mach number, outlet velocity, and outlet pressure of the C-D nozzle. Finally based on flow characteristics, Taguchi's DOE is analyzed.

2. Materials and Methods

This study involves the optimization of a C-D nozzle design for high-speed rockets through the Taguchi method for enhanced flow characteristics. The foremost step is to perform DOE by selecting and varying the design parameters of the nozzle. Then in the next step, based on DOE, the nozzles are designed in the SolidWorks software. Then CFD simulations are carried out using the ANSYS platform. In the final step, Taguchi's design is analyzed based on response variables of flow. The basic structure of this methodology is presented in Figure 1.

2.1. Taguchi DOE:

The Taguchi method was initially developed by Professor Genichi Taguchi [22]. It is a robust method used for optimization of parameters [23-30].To employ the Taguchi method, Minitab 21 software was used in this study which is majorly used for the optimization of different parameters[31]. Before performing DOE, the basic design of the nozzle, the constant design parameters, and the range of variable design parameters were selected based on the literature[2, 19]. As mentioned above, the variable design parameters are altered in three levels which are shown in Table I.

Based on these levels, Taguchi's L9 array was used for optimization. The core benefit of the Taguchi method is to reduce the number of runs for any experimental or computational study. The L9 orthogonal array reduced the computational runs to 9. The proposed L9 array containing nine combinations of design parameters is presented in Table II.

Table I. Variable Design Parameters

Level	Throat Diameter (m)	Convergent Angle	Divergent Angle
1	0.304	28°	10°
2	0.354	30°	15°
3	0.404	32°	20°

Table II. Taguchi's L9 Array Based on Variable Design Parameters

Run	Throat Diameter (m)	Convergent Angle	Divergent Angle
1	0.304	28°	10°
2	0.304	30°	15°
3	0.304	32°	20°
4	0.354	28°	15°
5	0.354	30°	20°
6	0.354	32°	10°
7	0.404	28°	20°
8	0.404	30°	10°
9	0.404	32°	15°

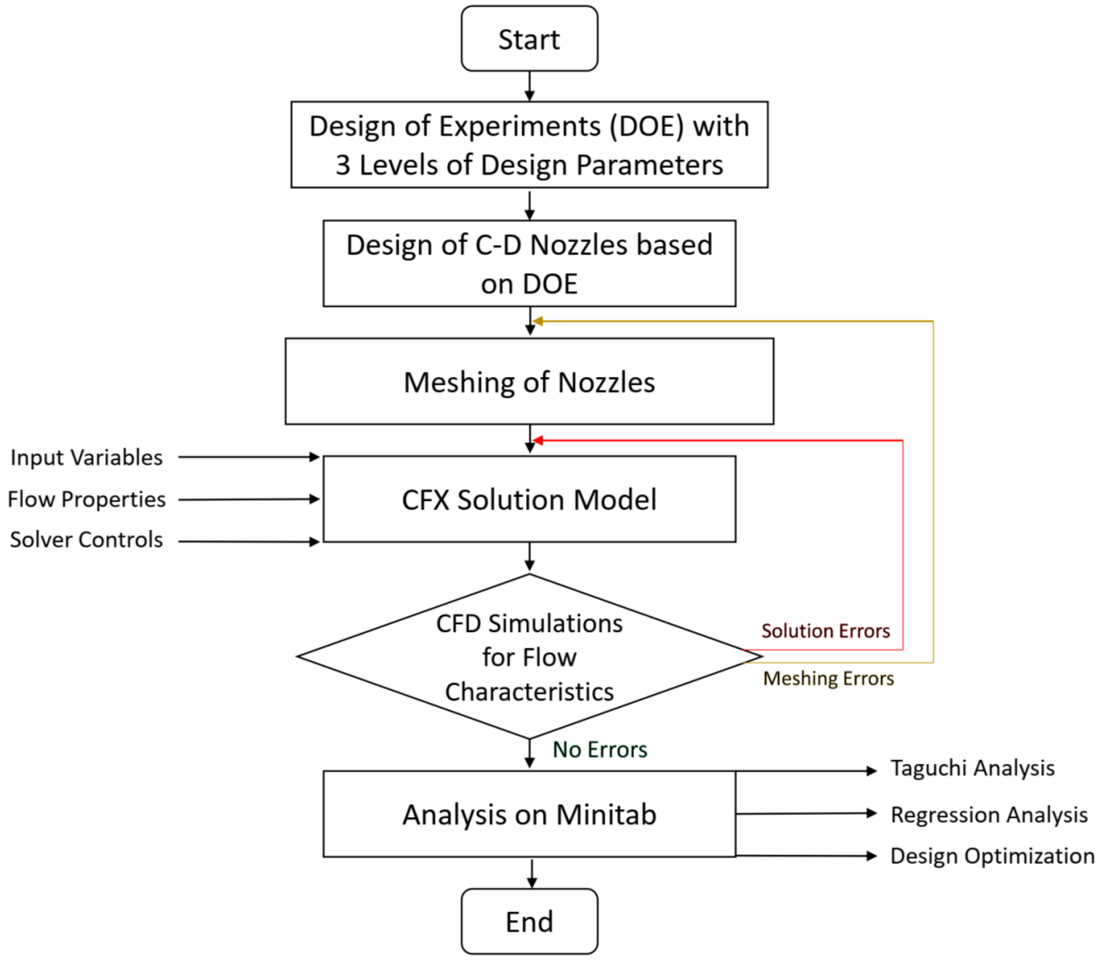

Figure 1. Procedure Involved in this Study

2.2. Designing 3D Models of C-D Nozzles:

Based on DOE, the C-D nozzles were designed using SolidWorks software. The other design considerations were according to the literature[2, 19]. All the geometrical design parameters (constant as well as variable) are given in Table III.

Based on these geometrical design parameters, nine conicalC-D nozzles were designed in SolidWorks software in 3D (because A 3D model provides a more realistic representation of flow physics), as shown in figure 2. Herein, the diameters of convergent and divergent sections were kept constant just to view the effects of angles and throat diameters.

2.3. CFD Simulations on ANSYS CFX:

In the next stage, the designed geometries of 3D C-D nozzles were imported into the ANSYS CFX module of Ansys Workbench one by one. Herein, the models were meshed to discretize the C-D nozzle flow domain into finite volumes. The mesh was selected to accurately capture all geometric details of the C-D nozzle while ensuring numerical stability[32-37]. Extremely small mesh sizes led to simulation errors, so an optimal mesh size was chosen to maintain computational accuracy without instability. Along with meshing, the named selection of inlet, outlet, and nozzle walls was also assigned in the meshing tab. The meshed model ofthe C-D nozzle is shown in Figure 3.

Table III. Design Parameters of C-D Nozzle Geometry

Design Parameters	Dimensions	Type
Convergent Diameter (mm)	1000	Constant
Divergent Diameter (mm)	861	Constant
Throat Diameter (mm)	304, 354, 404	Variable
Convergent Angle	28. 30, 32	Variable
Divergent Angle	10, 15, 20	Variable
Throat Fillet (mm)	228	Constant
Convergent Length	According to Angle	Variable
Divergent Length	According to Angle	Variable

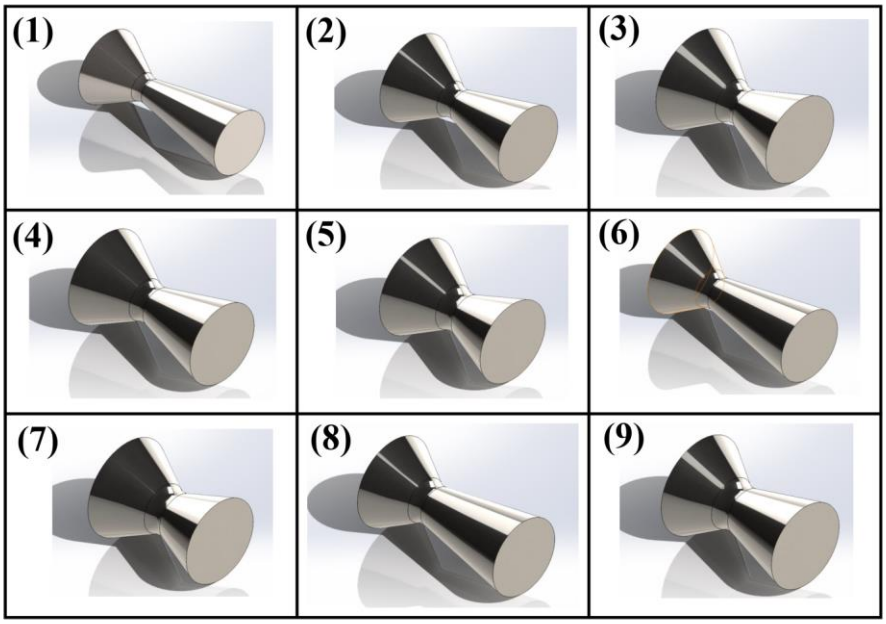

Figure 2. Designed C-D Nozzles Based on DOE Runs

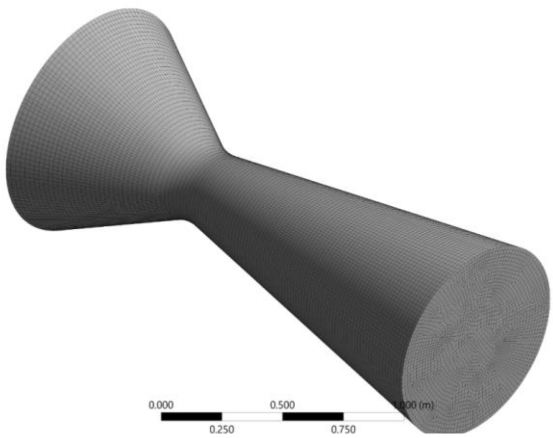

Figure 3. Meshed Model of Conical C-D Nozzle

After meshing, the CFX setup model was established. The problem type was selected as "single phase" and the fluid was set as "Air ideal gas". Steady-state analysis was performed using the Shear Stress Transport (SST) turbulence model with a reference pressure of 1 atm. According to the literature on liquid rocket engines, combustion chamber pressures range from 4.83 MPa to 24 MPa, with temperatures between 21K and 3600K[38].Based on these, in the CFX setup, the stagnation pressure at the inlet of the C-D nozzle was kept at 9.8 MPa whereas the inlet temperature was selected as 3500 K at the outlet, and the pressure was kept at0.101325 MPa (1 atm). Moreover, at the outlet of the nozzle, a pressure boundary condition was applied. The walls of the nozzle were kept as no-slip walls. 0.000001 (10^{-6}) residuals were kept for the simulation along with 1500 iterations. After completing the CFX setup model, the established model was solved. Any errors during the CFD simulation were corrected by going back to the basic setup or meshing and resolving the model. A summary of thermodynamics inputs and simulation criteria are shown in Tables IV and V respectively.

After the solution, the results were analyzed in the CFD-post processor of ANSYS CFX. A plane was added to the nozzle geometry. And on that plane, contours of different flow characteristics were obtained. For the current study, Mach number, velocity, and pressure contours were analyzed for all nine runs based on DOE.

3. Results and Discussions

3.1. CFD Results of Response Variables Across C-D Nozzle:

The flow behavior of exhaust air from the outlet of the rocket C-D nozzle was different for each run of the simulation. In most of the runs, shock occurred and the values of flow characteristics instead of increasing, suddenly dropped and vice versa. In the first run, the purpose of the C-D nozzle was completely fulfilled. The pressure inside the nozzle kept on decreasing from 9.8 MPa at the inlet of the nozzle to 0.0404 MPa at the outlet. Similarly, the velocity of hot gases at the inlet of the nozzle was about 120 m/s which increased significantly up to2225.688 m/s at the outlet. The behavior of the Mach number was also quite similar. At the inlet, the value of Mach number was recorded to be 0.1, which became exactly one at the throat of the C-D nozzle and further increased in the diverging section to 3.45 at the outlet describing the flow at the outlet to be perfectly supersonic. The contours of velocity, pressure, and Mach number for run one are presented in Figures 4, 5, and 6 respectively. A line plot of these characteristics is shown in Figure 7. Similar behavior was observed for run 4 where the maximum velocity value reached 2200 m/s and Mach number to 3.23 exhibiting supersonic flow. The pressure was dropped to 0.076 MPa. For run 3, the maximum value of velocity and Mach number reached 1981 m/s and 2.52 respectively. But near the outlet, shock was observed and both the values started to decrease. Although, the flow at the outlet was still supersonic with a Mach number of 1.88 and a velocity of 1687 m/s. This was due to the location of shock which was almost at the outlet.

Table IV. Thermodynamic Input Parameters

Parameter	Value/Type
Fluid Type	Air (Ideal Gas)
Reference Pressure	101325 Pa
Inlet Pressure	9.8 MPa
Inlet Temperature	3500 K
Outlet Pressure	101325 Pa

Table V. Simulation Criteria for CFD Solution

Parameter	Value/Type
Solver Type	CFX (Steady-State)
Turbulence Model	Shear Stress Transport (SST)
Boundary Condition (Inlet)	Pressure Inlet (9.8 MPa, 3500 K)
Boundary Condition (Outlet)	Supersonic Flow, 101325 Pa
Wall Condition	No-Slip Walls
Residuals	1×10^{-6} RMS
Iterations	1500

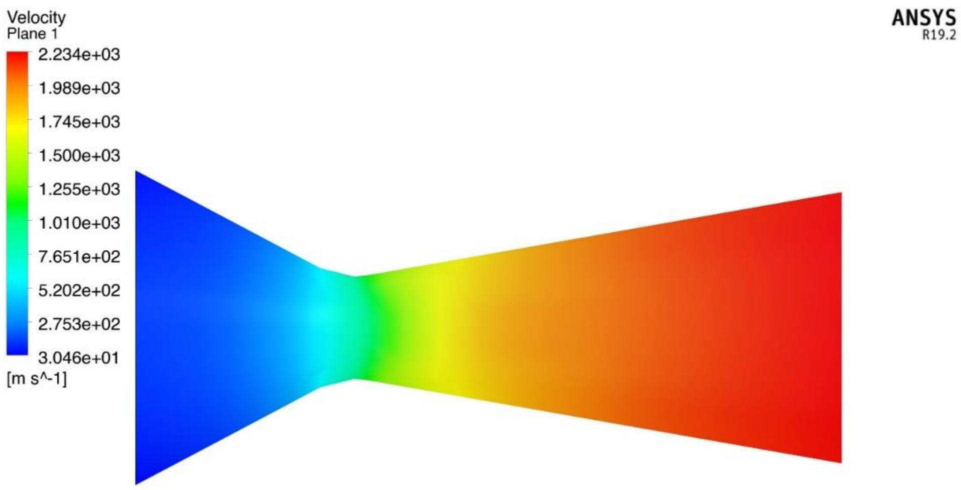

Figure 4. Velocity Contour of Run 1

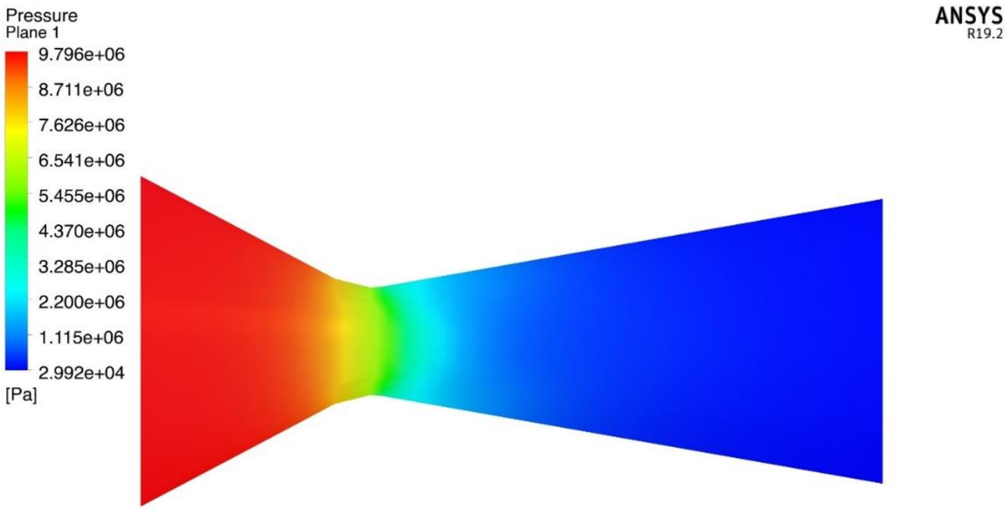

Figure 5. Pressure Contour of Run 1

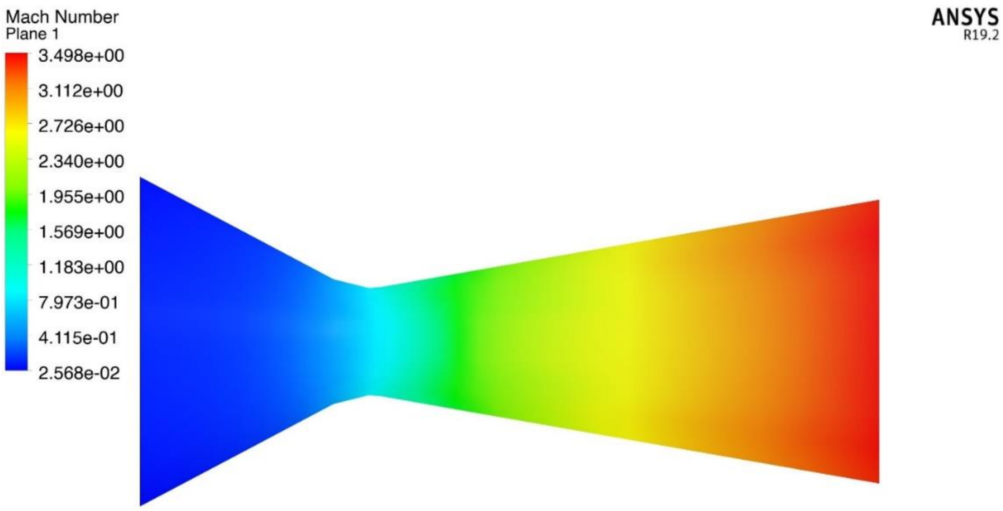

Figure 6. Mach Number Contour of Run 1

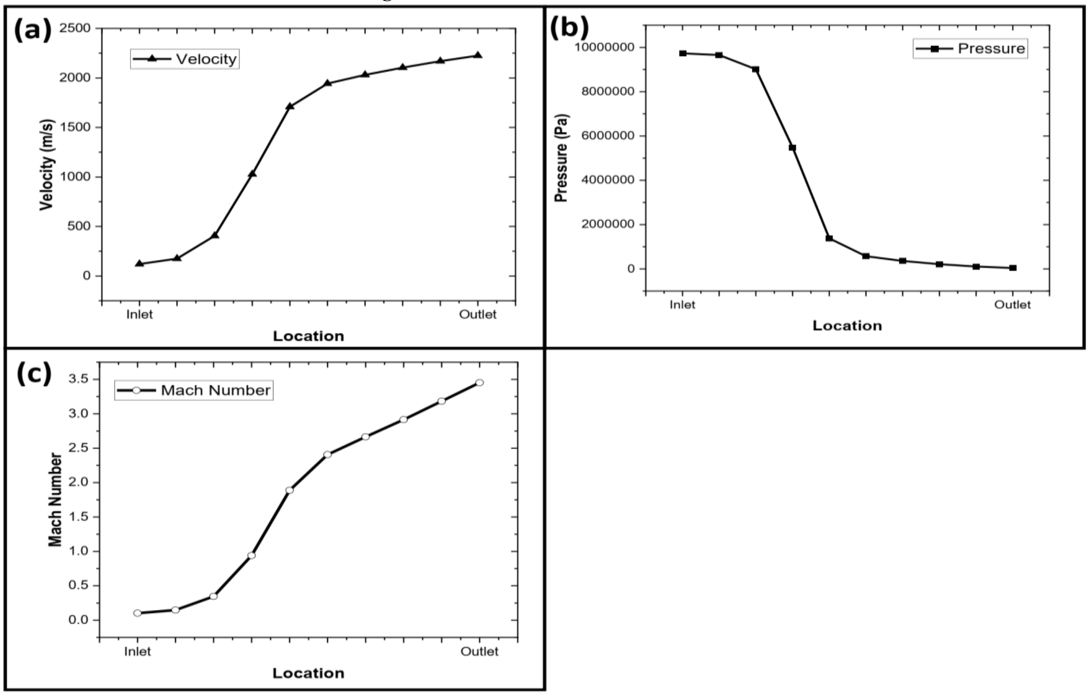

Figure 7. Properties Distribution for Run 1

In runs 2, 5, 7, and 8, after reaching the supersonic flow inside the nozzle, the Mach number and velocity decreased again along the length of the nozzle and exhibited subsonic flow at the outlet. These shocks decrease the efficiency of C-D nozzles and the outlet flow cannot be supersonic [18]. The location of the shock wave for all these nozzle geometries is different. This may be linked to the difference in the geometries of C-D nozzles due to variable length, throat diameter, and convergent and divergent angles. The shock wave location in run 2 is near the exit of the nozzle. In run 5, the shock happened just ahead of the throat and the Mach number and velocity started to decrease again pressure increased again after the shock wave. For run 7, the shock also happened near the throat of the C-D nozzle. However, the maximum reached Mach numbers for runs 2, 5, 7, and 8 are 2.97, 1.35, 1.23, and 1.15 respectively. The contour plots of velocity, pressure, and Mach number for run 2 are presented in Figures 8, 9, and 10 respectively whereas the line plot for all these parameters is given in Figure 11.

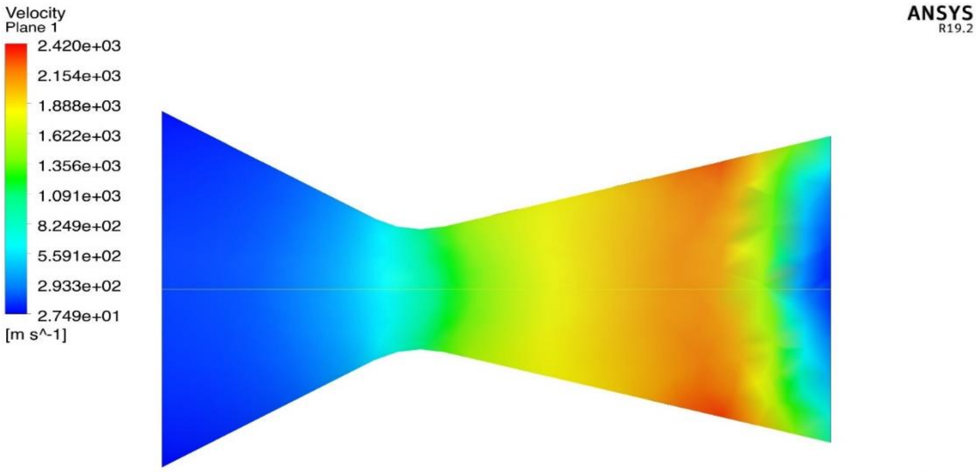

Figure 8. Velocity Contour of Run 2

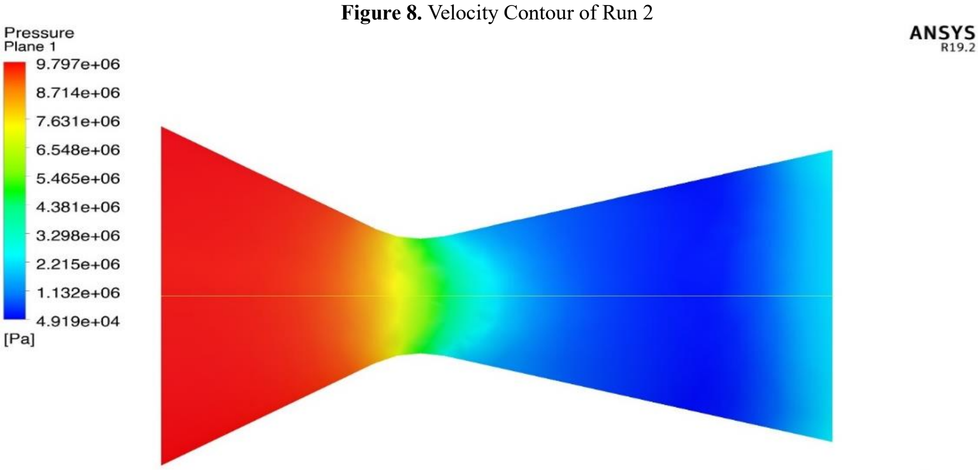

Figure 9. Pressure Contour of Run 2

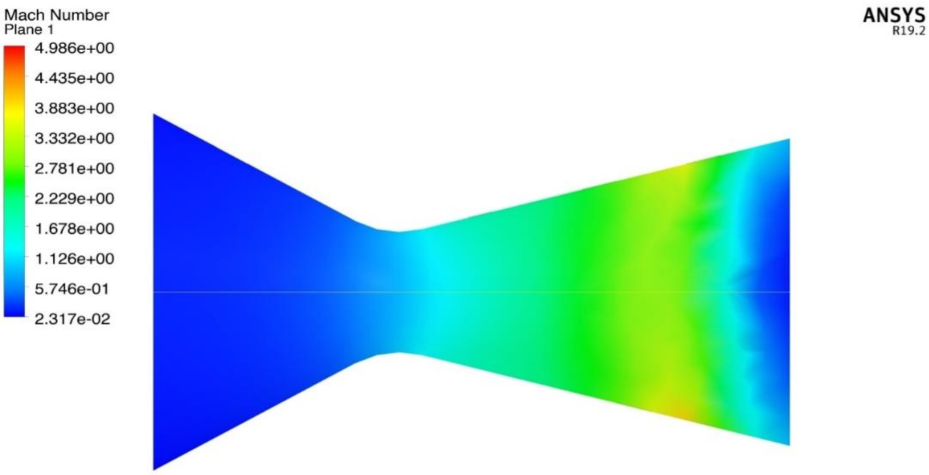

Figure 10. Mach Number Contour of Run 2

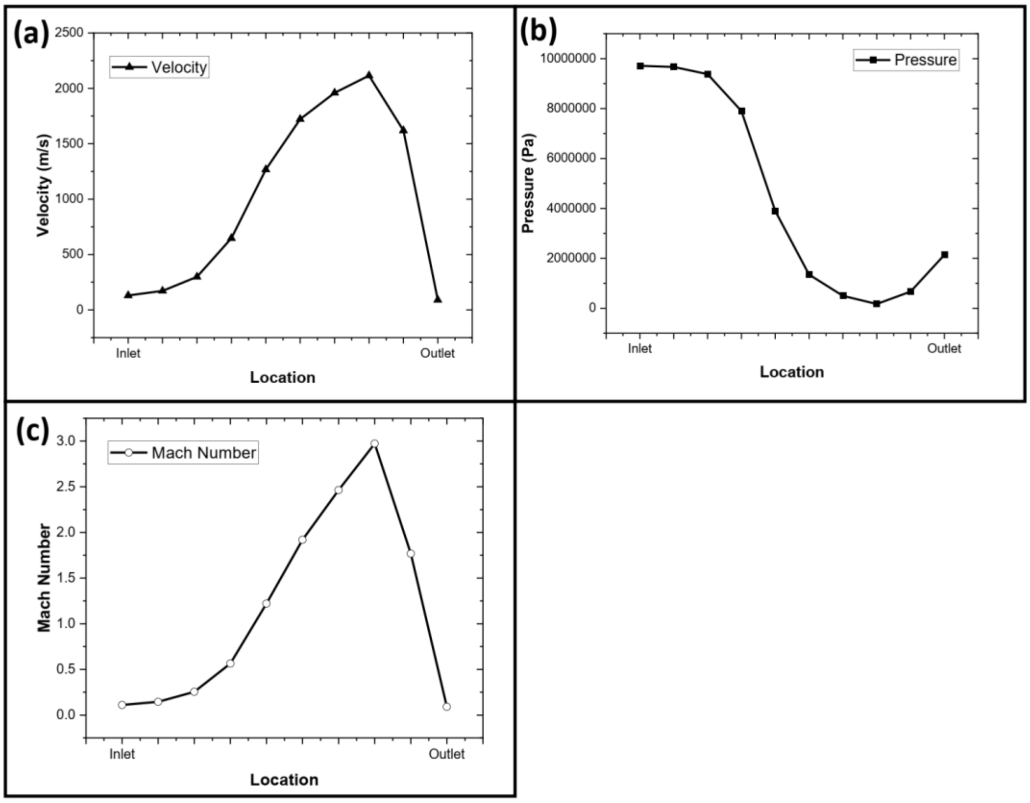

Figure 11. Properties Distribution for Run 2

For runs 6 and 9, the flow never reached to supersonic conditions. Until the throat, the Mach number started to increase but again decreased along the length. The flow in this range remained subsonic. It was observed that nozzle geometry configurations having larger throat diameters showed lower Mach number and velocity values. Better flow characteristics were obtained for run 1.

3.2. Taguchi's Analysis:

Taguchi's S/N ratio or signal-to-noise ratio is the ratio of the mean value (signal) to the standard deviation (noise)[39]. It is the measure of the deviation of response variables from the target value[40].There are three standards of S/N ratios which include larger is better, nominal is better, and smaller is better. In the current study, high velocity and high Mach number are required at the outlet of the rocket C-D nozzle. So, for these two response variables, the "largeris better" S/N ratio was incorporated. However, for pressure, the desired value should be decreased across the length of the nozzle. So, for pressure values, the S/N ratio of "smaller is better" was selected. The equations to calculate S/N ratios for "larger is better" "smaller is better" and "nominal is best" are provided below in equations 1, 2, and 3 respectively.

For "larger is better"

$$\frac{S}{N} = -10\ log\left(\frac{1}{n}\sum_{i=1}^{n}\left(\frac{1}{R^2}\right)\right) \qquad (1)$$

For "smaller is better"

$$\frac{S}{N} = -10\ \log\left(\frac{1}{n}\sum_{i=1}^{n}(R^2)\right) \qquad (2)$$

For "nominal is best"

$$\frac{S}{N} = 10\log\left(\frac{R^2}{s^2}\right) \qquad (3)$$

Here "R" depicts the response variable under discussion whereas "n" represents the number of trials for a run. On the other hand, "s" depicts the standard deviation used in the "nominal is best" S/N ratio. In the current study, the S/N ratios for all the analyzed response variables (i.e. output flow characteristics) were calculated through Taguchi analysis on the Minitab software. For all the standard S/N ratio types, parameters with the highest S/N ratio value are considered optimal.

3.2.1. Exit Flow Velocity:

Although in most of the geometrical configurations of C-D nozzles analyzed in this study, the value of velocity increased to a certain limit in different locations of the nozzles across their length, the flow velocity at the outlet of the C-D nozzle determines the performance and efficiency of the rocket. Based on this, response parameters at the outlet of the C-D nozzle were selected for the Taguchi analysis. The exit velocity of the C-D nozzle and S/N ratios associated with them for all nine runs are presented in Table VI below.

Table VI. Exit Velocity and S/N Ratios of Exit Velocityof all Runs

Run	Outlet Velocity (m/s)	S/N Ratio
1	2225.69	66.9493
2	89.88	39.0734
3	1687.86	64.5467
4	2200.18	66.8492
5	992.41	59.9338
6	19.91	25.9799
7	816.37	58.2378
8	492.89	53.8550
9	3.63	11.1863

Table VII. Response of S/N Ratios for Exit Velocity

Level	Throat Diameter (mm)	Convergent Angle	Divergent Angle
1	56.86	64.01	48.93
2	50.92	50.95	39.04
3	41.09	33.90	60.91
Delta	15.76	30.11	21.87
Rank	3	1	2

The higher velocity is desired at the outlet of the rocket C-D nozzle. The S/N ratio is also highest for the run having the highest velocity among all nine runs i.e. run 1. The response table for the S/N ratio of exit velocity is provided in Table VII and the S/N ratio plot is provided in Figure 12.

From the results, it is evident that the convergent angle is the most influential parameter that shapes the flow characteristics of the rocket C-D nozzle. The percentage contribution of convergent angle is around 45%. S/N ratios determine the optimal settings of the response parameters. A higher S/N ratio of a response variable determines that the parameter associated with that ratio would provide better results in terms of the response variable. In this case, higher SN ratios are observed at 0.304 m throat diameter, 28^o convergent angle and 20^o divergent angle. From the S/N plot, it can be concluded that the optimal design conditions for better and higher exit velocity are 304 mm throat diameter, 28^o convergent angle, and 20^o divergent angle.

To predict the exit velocity of the nozzle, regression analysis was also performed on Minitab software. Equation 4 shows the regression equation for the prediction of outlet velocity in m/s.

$$\text{Outlet Velocity} = 12571 - 8968\ \text{Throat Diameter} - 294\ \text{Convergent Angle} + 25.3\ \text{Divergent Angle} \quad (4)$$

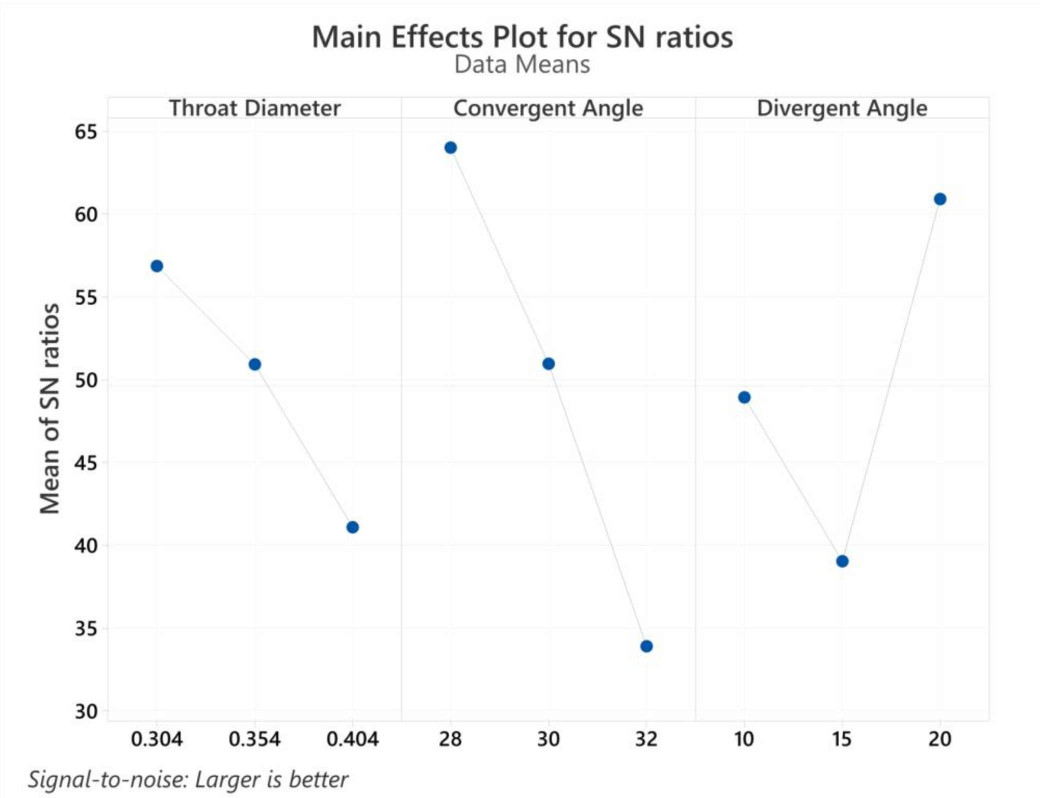

Figure 12. S/N Ratio Plot for Exit Velocity

3.2.2. Exit Flow Pressure:

From the results of CFD simulations, the pressure at the outlet of the C-D nozzle just before leaving the nozzle was examined and is presented in Table VI. The pressure trend follows an inverse relationship with velocity. For those nozzle geometries where shock did not happen, the pressure decreased with the increase in velocity. Similarly, the lowest pressure was observed at the outlet for run 1. As desired, the “smaller is better” S/N ratio calculation has been done using equation 2. The corresponding S/N ratios of exit pressure for all nine runs are presented in Table VIII.

Table VIII. Exit Pressure and S/N Ratios of Exit Pressure of all Runs

Run	Exit Pressure (Pa)	S/N Ratio
1	40430	-92.134
2	2137517	-126.598
3	703347	-116.943
4	76105	-97.628
5	4939467	-133.874
6	9797819	-139.823
7	6107498	-135.717
8	7064767	-136.982
9	9799940	-139.824

Details of responses of the S/N ratio for exit pressure are given in TableIX. It can be observed in the table that the difference between the largest and smallest value is the highest for throat diameter i.e. 25.6 termed as delta. Based on this highest value, throat diameter is ranked as the most effective parameter that can influence the desired outcome i.e. decreased pressure in our case. Convergent angle is ranked number 2 after the throat diameter whereas divergent angle stands last among all the input design parameters.

Table IX. Response of S/N Ratios for Exit Pressure

Level	Throat Diameter	Convergent Angle	Divergent Angle
1	-111.9	-108.5	-123.0
2	-123.8	-132.5	-121.4
3	-137.5	-132.2	-128.8
Delta	25.6	24.0	7.5
Rank	1	2	3

Figure 13 shows the S/N ratio plots for pressure at the outlet of the rocket C-D nozzle. An abrupt fall in the S/N ratio line of throat diameter validates the number rank of throat diameter for influencing the pressure to be decreased. The S/N plot of exit pressure also defines the optimized set of design parameters for the rocket C-D nozzle that can provide the lowest exit pressure if the same design and boundary conditions are used. That optimized set of design parameters is a throat diameter of 0.304 m, 28º convergent angle, and 15º divergent angle. This set would help in attaining the desired response of pressure in the rocket C-D nozzle.

Equation 5 shows the regression equation to predict the pressure at the exit of the C-D nozzle using the given design parameters.

Outlet Pressure (Pa)=-51805063 + 66969703 Throat Diameter+ 1173089 Convergent Angle- 171757 Divergent Angle (5)

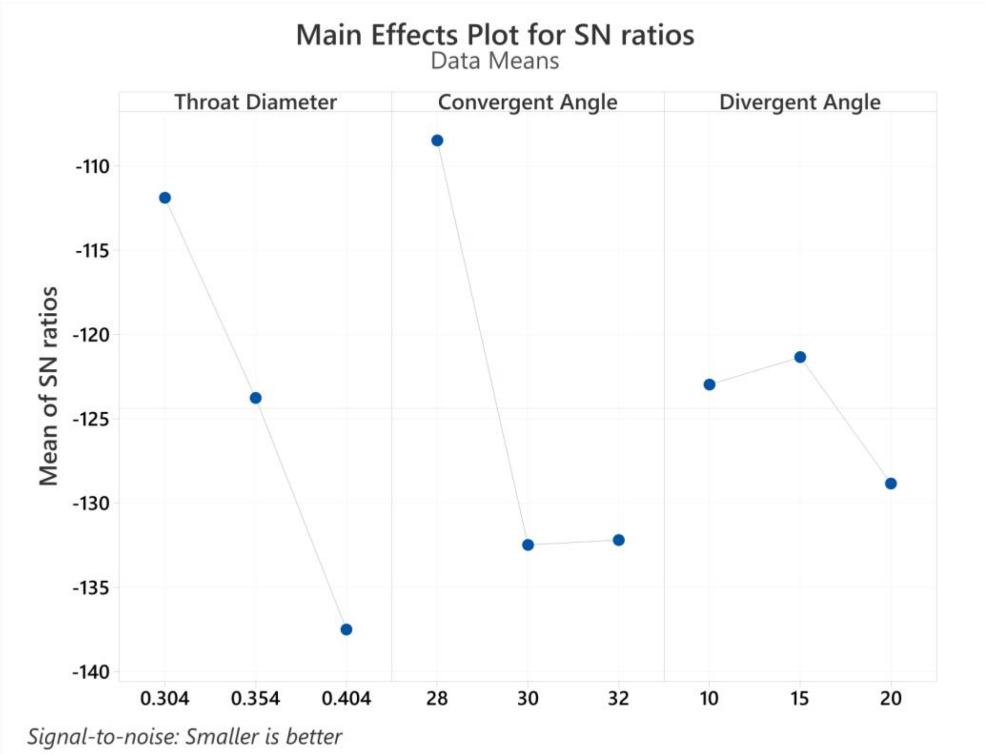

Figure 13. S/N Ratio Plot for Exit Pressure

3.2.3. Exit Mach Number:

For the supersonic flow of air, the exit of the C-D nozzle, the Mach number at the outlet of the nozzle must be greater than 1. The trend of the Mach number is perfectly associated with the velocity. With the increase in velocity, the Mach number also increases. As mentioned above, for normal operating conditions of the C-D nozzle without shock waves, the flow is subsonic in the converging portion, sonic in the throat, and becomes supersonic in the diverging portion and stays supersonic till the exhaust. The Mach numbers for all the nine runs included in DOE are presented in Table X. Apart from runs 6 and 9, the runs having a Mach number less than 1 at the outlet of the nozzle had developed shock waves during the passage of exhaust gases along the length of the C-D nozzle. Like velocity, the "larger is better" S/N ratio has been applied to the Mach number values.

Responses of S/N ratios for exit Mach number are provided in Table XI. For this response, the delta value is highest for the converging angle. It means that for the desired response of a high Mach number at the outlet of the C-D nozzle, convergent angle is the most influential parameter. Rank-wise, divergent is the second most influential, and throat diameter is the third number.

The S/N ratio plot for the outlet Mach number confirms the first rank of convergent angle in determining the Mach number at the outlet of rocket C-D nozzle as shown in Figure 14. This plot also provides optimized design parameters that can yield a high Mach number at the outlet of the C-D nozzle operating under the assessed conditions. Here too, the parameter value having the highest S/N ratio is selected as the optimized one. Based on exit Mach number, 0.304 m throat diameter, 28° convergent angle, and 20° divergent angle are provided as optimized parameters to achieve supersonic flow at the outlet of rocket C-D nozzle.

The regression equation for estimation of exit Mach number in terms of throat diameter, convergent angle, and divergent angle is shown below in equation 6.

$$\text{Outlet Mach Number} = 20.43 - 14.26\ \text{Throat Diameter} - 0.466\ \text{Convergent Angle} - 0.0128\ \text{Divergent Angle} \quad (6)$$

Table X. Exit Mach Number and S/N Ratios of Exit Mach Number of all Runs

Run	Mach Number	S/N Ratio
1	3.45263	10.7630
2	0.09025	-20.8908
3	1.88437	5.5033
4	3.32380	10.4327
5	0.90239	-0.8921
6	0.01679	-35.5014
7	0.72352	-2.8110
8	0.42383	-7.4561
9	0.00306	-50.2943

Table XI. Response of S/N Ratios for Exit Mach Number

Level	Throat Diameter	Convergent Angle	Divergent Angle
1	-1.5415	6.1282	-10.7315
2	-8.6536	-9.7463	-20.2508
3	-20.1872	-26.7641	0.6001
Delta	18.6457	32.8924	20.8509
Rank	3	1	2

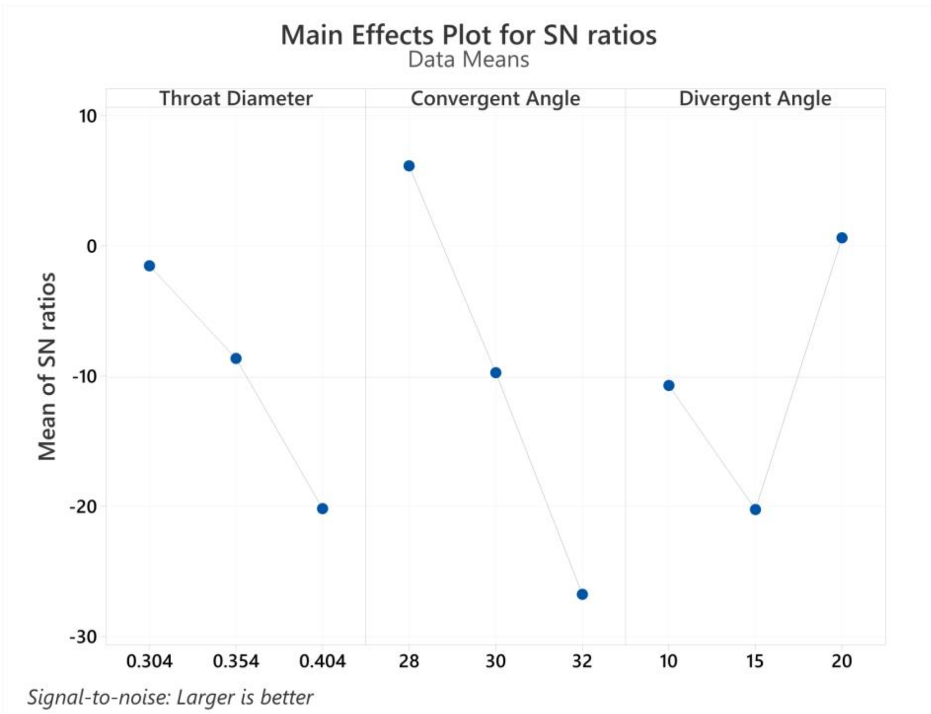

Figure 14. S/N Ratio Plot for Exit Mach Number

3.3. Parametric Optimization:

Based on Taguchi analysis, two different sets of rocket C-D nozzle design parameters have been evaluated i.e. 0.304 m throat diameter, 28º convergent angle, and 20º divergent angle for enhanced velocity and the Mach number and, 0.304 m, 28º convergent angle and 15º divergent angle for enhanced pressure value at the outlet of C-D nozzle. However, it may be assumed that an optimized set of parameters involving 0.304 m throat diameter, 28º convergent angle, and 20º divergent angle may provide better results for all the three input design parameters analyzed in this study. A divergent angle of 20º may slightly reduce the gross thrust coefficient (with these effects being negligible)[41] as compared to 15º but at the same time, according to Taguchi analysis, it can provide better values of the Mach number and velocity at the outlet for the rocket C-D nozzle having the operating conditions presented in this study. Based on these findings, it is concluded that among the two aforementioned sets of design parameters, 0.304 m throat diameter, 28º convergent angle, and 20º divergent angle may provide better results at the outlet of rocket C-D nozzle as desired.

4. Conclusions

This present study explores the design optimization of a rocket C-D nozzle by varying throat diameter, convergent angle, and divergent angle at three levels based on Taguchi's L9 orthogonal array. Based on DOE, the geometrical models of C-D nozzles were designed in SolidWorks and those models were imported into the ANSYS CFX module for CFD analysis of those nozzle configurations. Outlet velocity, outlet pressure, and outlet Mach number were the response variables of this study. Using proper S/N ratios in the Taguchi method, the results of all nine runs were evaluated and optimized along with regression analysis. The key findings of this study are presented below:

1. CFD analysis can be a good alternative to expensive and complex experimental investigation for the initial analysis of large C-D nozzles for rockets. However, experimental validation is still necessary for a true and comprehensive picture of the flow characteristics of C-D nozzles.
2. The throat diameter significantly influences the mass flow rate, which in turn affects the flow characteristics at the nozzle outlet. In this study, a throat diameter of 0.304 m provided better results for all response variables at the outlet compared to 0.354 m and 0.404 m.
3. A convergent angle of 28º provided better results for all three response variables under the specified operating conditions. This angle helps accelerate the flow efficiently, ensuring that the Mach number reaches Ma = 1 at the throat, a crucial condition for optimal nozzle performance.
4. Optimized set of design parameters includes 0.304 m throat diameter, 28º convergent angle, and 20º divergent angle. These parameters have the capacity to provide supersonic flow at the outlet (with high velocity and decreased pressure) of the C-D nozzle operating under the conditions presented in this study.
5. As the literature suggests, a sudden drop in the Mach number and velocity was observed for several designed nozzle geometries due to the formation of shock waves. With these shock waves, pressure after dropping to a certain length of nozzle again started to rise in those nozzles.

5. Limitations and Future Prospects

The analysis and simulations performed in this study are done on the base design presented by Madhu et al. and Meena et al. So, these results might not be applicable to other designs or geometries of nozzles. Other designs of C-D nozzles can be analyzed by following the same procedure presented in this study for optimization. Some assumptions are also taken during this research which might limit the results as well. These assumptions include the perfect "ideal gas" behavior of exhaust gases which might not be the case in practical applications. Moreover, flow is assumed to be steady-state in this study which might also fluctuate in some instances. In the future, design analysis based on practical rocket design parameters can be performed. Moreover, CFD simulations on other commercially available software can also be done and compared with these.

References

[1] A. Bhaskar and M. K. Sahu, "Numerical investigation on performance of convergent–divergent nozzle with multi-inlet combustion chamber of a rocket engine," *Heat Transfer,* vol. 51, no. 1, pp. 5-21, 2022/01/01 2022, doi: https://doi.org/10.1002/htj.22296.

[2] L. Meena, M. S. Niranjan, Aman, Gautam, Gagandeep, G. Kumar, and M. Zunaid, "Numerical study of convergent-divergent nozzle at different throat diameters and divergence angles," *Materials Today: Proceedings,* vol. 46, pp. 10676-10680, 2021/01/01/ 2021, doi: https://doi.org/10.1016/j.matpr.2021.01.432.

[3] N. Yu, R. Jourdain, M. Gourma, and P. Shore, "Analysis of De-Laval nozzle designs employed for plasma figuring of surfaces," *The International Journal of Advanced Manufacturing Technology,* vol. 87, no. 1, pp. 735-745, 2016/10/01 2016, doi: 10.1007/s00170-016-8502-y.

[4] N. Goodman, B. J. Leege, and P. E. Johnson, "An improved de Laval nozzle experiment," *International Journal of Mechanical Engineering Education,* vol. 50, no. 2, pp. 513-537, 2022/04/01 2021, doi: 10.1177/03064190211034165.

[5] Y. Zhu and P. Jiang, "Experimental and analytical studies on the shock wave length in convergent and convergent–divergent nozzle ejectors," *Energy Conversion and Management,* vol. 88, pp. 907-914, 2014/12/01/ 2014, doi: https://doi.org/10.1016/j.enconman.2014.09.023.

[6] D. Papamoschou, A. Zill, and A. Johnson, "Supersonic flow separation in planar nozzles," *Shock Waves,* vol. 19, no. 3, pp. 171-183, 2009/07/01 2009, doi: 10.1007/s00193-008-0160-z.

[7] M. Al-Ajlouni, "An Automaic Method for Creating the Profile of Supersonic Convergent-Divergent Nozzle," *JJMIE,* vol. 4, no. 3, 2010.

[8] N. Husnain, F. A. Siddiqui, R. Ahmad, S. M. A. Bukhari, I. Nasir, M. F. Shafi, and M. A. Hanif, "Experimental and Computational study of the most Influential Parameters of a Lab-Scale Forced Draft Cooling Tower by considering

different number of Packing Ribs," *Technical Journal,* vol. 27, no. 04, pp. 20-27, 2022.

[9] R. Ramesh Kumar and Y. Devarajan, "CFD simulation analysis of two-dimensional convergent-divergent nozzle," *International Journal of Ambient Energy,* vol. 41, no. 13, pp. 1505-1515, 2020/11/09 2020, doi: 10.1080/01430750.2018.1517683.

[10] M. Nakagawa, M. S. Berana, and A. Kishine, "Supersonic two-phase flow of CO2 through converging–diverging nozzles for the ejector refrigeration cycle," *International Journal of Refrigeration,* vol. 32, no. 6, pp. 1195-1202, 2009/09/01/ 2009, doi: https://doi.org/10.1016/j.ijrefrig.2009.01.015.

[11] J. Zhu and S. Elbel, "CFD simulation of vortex flashing R134a flow expanded through convergent-divergent nozzles," *International Journal of Refrigeration,* vol. 112, pp. 56-68, 2020/04/01/ 2020, doi: https://doi.org/10.1016/j.ijrefrig.2019.12.005.

[12] E. Zhalehrajabi, N. Rahmanian, and N. Hasan, "Effects of mesh grid and turbulence models on heat transfer coefficient in a convergent–divergent nozzle," *Asia-Pacific Journal of Chemical Engineering,* vol. 9, no. 2, pp. 265-271, 2014/03/01 2014, doi: https://doi.org/10.1002/apj.1767.

[13] B. D. Das, R. Sardar, S. Sarkar, and N. K. Manna, "Compressible Flow Through Convergent–Divergent Nozzle," in *Theoretical, Computational, and Experimental Solutions to Thermo-Fluid Systems*, Singapore, M. Palanisamy, V. Ramalingam, and M. Sivalingam, Eds., 2021// 2021: Springer Singapore, pp. 345-353.

[14] A. K. Ababneh, A. M. Jawarneh, H. M. Tlilan, and M. K. Ababneh, "The effects of the secondary fluid temperature on the energy transfer in an unsteady ejector with a radial-flow diffuser," *Heat and Mass Transfer,* vol. 46, no. 1, pp. 95-105, 2009/11/01 2009, doi: 10.1007/s00231-009-0547-0.

[15] C. G. AK Ababaneh, AM Jawarneh, H Tlilan, "Investigation of the Mach number effects on fluid-to-fluid interaction in an unsteady ejector with a radial-flow diffuser," *Jordan Journal of Mechanical and Industrial Engineering,* vol. 3, no. 2, 2009.

[16] B. Douaiba, F. Baghlad, and M. Hamel, "Analysis of compressible flow at the outlet of a convergent – divergent nozzle," *Desalination and Water Treatment,* vol. 279, pp. 160-163, 2022/12/01/ 2022, doi: https://doi.org/10.5004/dwt.2022.29102.

[17] S. A. Khan, O. M. Ibrahim, and A. Aabid, "CFD analysis of compressible flows in a convergent-divergent nozzle," *Materials Today: Proceedings,* vol. 46, pp. 2835-2842, 2021/01/01/ 2021, doi: https://doi.org/10.1016/j.matpr.2021.03.074.

[18] P. Vadivelu, G. Senthilkumar, G. Sivaraj, D. Lakshmanan, and N. Uday Ranjan Goud, "Performance analysis of CD nozzle," *Materials Today: Proceedings,* vol. 64, pp. 620-631, 2022/01/01/ 2022, doi: https://doi.org/10.1016/j.matpr.2022.05.148.

[19] B. P. Madhu, G. Mahendramani, and K. Bhaskar, "Numerical analysis on flow properties in convergent – Divergent nozzle for different divergence angle," *Materials Today: Proceedings,* vol. 45, pp. 207-215, 2021/01/01/ 2021, doi: https://doi.org/10.1016/j.matpr.2020.10.419.

[20] R. Kore, S. Patil, V. Victor, S. Suresh, and D. K. Bajaj, "CFD Investigation in CD Nozzle at Different Convergence Angles and Constant Divergence Angle and Throat Diameter," in *2021 IEEE Pune Section International Conference (PuneCon)*, 16-19 Dec. 2021 2021, pp. 1-7, doi: 10.1109/PuneCon52575.2021.9686491.

[21] A. Aabid and S. A. Khan, "Investigation of High-Speed Flow Control from CD Nozzle Using Design of Experiments and CFD Methods," *Arabian Journal for Science and Engineering,* vol. 46, no. 3, pp. 2201-2230, 2021/03/01 2021, doi: 10.1007/s13369-020-05042-z.

[22] M. Soori and M. Asmael, "A review of the recent development in machining parameter optimization," *Jordan Journal of Mechanical and Industrial Engineering,* vol. 16, no. 2, pp. 205-223, 2022.

[23] T. Tran and H. Dai Vu, "Multi-objective optimization of CNC milling parameters of 7075 aluminium alloy using response surface methodology," *JJMIE,* vol. 17, no. 3, 2023.

[24] A. H. Q. Ayun, J. Triyono, and E. Pujiyanto, "Optimization of injection molding simulation of bioabsorbable bone screw using Taguchi method and particle swarm optimization," *Jordan Journal of Mechanical and Industrial Engineering,* vol. 16, no. 2, pp. 319-325, 2022.

[25] H. M. Abdu, S. M. Tahaa, A. Wazeer, A. Abd El-Mageed, and M. M. Mahmoud, "Application of Taguchi Method and Response Surface Methodology on Machining Parameters of Al MMCs 6063-TiO 2," *Jordan Journal of Mechanical and Industrial Engineering,* vol. 17, no. 4, 2023.

[26] T. Alsardia and L. Lovas, "Investigation of the Effect of the Surface Treatment and Lubrication During Repeated Tightening on the Nut Coefficient of a Bolted Joint Using the Taguchi Method," *Jordan Journal of Mechanical and Industrial Engineering,* vol. 18, no. 1, 2024.

[27] H. Gowda and R. HN, "Study on Strontium and Sodium Modification Elements on Microstructure, Mechanical, Wear and Fracture Behavior of Al7075 Alloy by Taguchi Technique," *Jordan Journal of Mechanical and Industrial Engineering,* vol. 18, no. 1, 2024.

[28] T. K. IBRAHIM, J. THADDAEUS, C. A. POPOOLA, I. ILIYASU, and A. A. ALABI, "Improvement of Wear Rate Properties of a Brown Pumice and Coal Ash Particulates Reinforced Aluminum Composite for Automobile Brake Manufacturing, Through Optimization and Modelling," *Jordan Journal of Mechanical and Industrial Engineering,* vol. 18, no. 4, 2024.

[29] H. Alzyod and P. Ficzere, "Thermal Evaluation of Material Extrusion Process Parameters and Their Impact on Warping Deformation," *Jordan Journal of Mechanical and Industrial Engineering,* vol. 17, no. 4, 2023.

[30] T. Hakmi, A. Hamdi, A. Laouissi, H. Abderazek, S. Chihaoui, and M. A. Yallese, "Mathematical Modeling Using ANN Based on k-fold Cross Validation Approach and MOAHA Multi-Objective Optimization Algorithm During Turning of Polyoxymethylene POM-C," *Jordan Journal of Mechanical and Industrial Engineering,* vol. 18, no. 1, 2024.

[31] S. M. A. Bukhari, N. Husnain, F. A. Siddiqui, M. T. Anwar, A. A. Khosa, M. Imran, T. H. Qureshi, and R. Ahmad, "Effect of laser surface remelting on Microstructure, mechanical properties and tribological properties of metals and alloys: A review," *Optics & Laser Technology,* vol. 165, p. 109588, 2023/10/01/ 2023, doi: https://doi.org/10.1016/j.optlastec.2023.109588.

[32] S. M. A. Bukhari, A. Naveed, N. Husnain, F. A. Siddiqui, M. F. Zaman, A. Ahmad, R. Ahmad, and N. Wajahat, "Computational study of mechanical behavior of Ti6Al4V-coated and aluminium-coated 316L stainless steel alloy under linear and cyclic loading," *Technical Journal,* vol. 28, no. 03, pp. 12-24, 2023.

[33] M. F. Zaman, S. M. A. Bukhari, N. Husnain, Z. Abbas, A. Ayyub, M. F. Najmi, A. Manan, and M. Zahid, "Effect of zirconium carbide coating on thermal behavior of heavy duty V12 diesel engine using finite element method," *Engineering Research Express,* vol. 6, no. 2, p. 025549, 2024/05/30 2024, doi: 10.1088/2631-8695/ad4f51.

[34] A. Naveed, S. M. A. Bukhari, N. Husnain, N. Balouch, S. Noor, W. Ahmad, S. Sarfraz, N. Wajahat, and F. A. Siddiqui, "Structural Integrity and Cost Analysis of a Connecting Rod for Articulated Robotic Arm Using Various Stainless Steel

and Aluminium Alloys," *Technical Journal*, vol. 29, no. 02, pp. 24-34, 2024.

[35] M. Abdullah, S. M. A. Bukhari, N. Husnain, M. F. Zaman, A. Tariq, F. A. Siddiqui, R. Ahmad, and M. D. Nasir, "Design, analytical and computational analysis, and development of a high-precision CNC spindle for a vertical machining center," *Engineering Research Express*, vol. 6, no. 3, p. 035568, 2024.

[36] S. M. Bukhari, S. A. Gardezi, N. Husnain, R. Ahmad, M. F. Zaman, R. Qurashi, and N. Baloch, "Modelling and simulation of cathodic protection using magnesium sacrificial anode for steel Bent-Y-Pipe in seawater environment."

[37] S. M. A. Bukhari, R. Qurashi, N. Husnain, M. A. Sadiq, M. Q. Zafar, M. T. Anwar, S. Abbas, F. A. Siddiqui, and S. Sarfraz, "Response Surface Methodology-Based Optimization of Coating Material, Coating Thickness, and Diameter of Dental Implant for Enhanced Mechanical Behavior Using Finite Element Method," *Advanced Engineering Materials*, vol. 26, no. 24, p. 2401729, 2024.

[38] J. Halchak, "Spacecraft Materials," in *Encyclopedia of Materials: Science and Technology*, K. H. J. Buschow *et al.* Eds. Oxford: Elsevier, 2001, pp. 8755-8758.

[39] N. Ghosh, P. K. Pal, and G. Nandi, "GMAW dissimilar welding of AISI 409 ferritic stainless steel to AISI 316L austenitic stainless steel by using AISI 308 filler wire," *Engineering Science and Technology, an International Journal*, vol. 20, no. 4, pp. 1334-1341, 2017/08/01/ 2017, doi: https://doi.org/10.1016/j.jestch.2017.08.002.

[40] M. Akbari, P. Asadi, M. K. Besharati Givi, and G. Khodabandehlouie, "13 - Artificial neural network and optimization," in *Advances in Friction-Stir Welding and Processing*, M. K. B. Givi and P. Asadi Eds.: Woodhead Publishing, 2014, pp. 543-599.

[41] M. H. Hamedi-Estakhrsar, H. Mahdavy-Moghaddam, and M. Jahromi, "Investigation of effects of convergence and divergence half-angles on the performance of a nozzle for different operating conditions," *Journal of the Brazilian Society of Mechanical Sciences and Engineering*, vol. 40, no. 7, p. 353, 2018/06/22 2018, doi: 10.1007/s40430-018-1271-9.